Conductance Behavior of Tetraphenyl-Aza-BODIPYs

Andrei Markin[a,Z], Ali K. Ismael,[b,c,Z]* Ross J. Davidson,[a]* David C. Milan,[d,Z] Richard J. Nichols,[d]* Simon J. Higgins,[d] Colin J. Lambert,[b] Yu-Ting Hsu,[a] Dmitry S. Yufit,[a] Andrew Beeby,[a]*.

[a]*Department of Chemistry, Durham University, South Rd, Durham, DH1 3LE, UK*

[b]*Department of Physics, University of Lancaster, Lancaster LA1 4YB, U.K.*

[c]*Department of Physics, College of Education for Pure Science, Tikrit University, Tikrit, Iraq*

[d]*Department of Chemistry, University of Liverpool, Crown St, Liverpool, L69 7ZD, UK*

[Z]*These Authors contributed equally to this work*

ABSTRACT: We studied the electrical conductance of single-molecule junctions formed from molecular wires with 4 anchor groups. Three tetraphenyl-aza-BODIPYs with 4 or 2 thiomethyl anchor groups were synthesized and their single-molecule conductance measured using break-junction-STM. Using DFT based calculations these compounds were shown to contain a combination of constructive and destructive quantum interference, depending on the molecule's connectivity in the junction. A scissor correction is employed to obtain the corrected HOMO-LUMO gaps and a tight binding model (TBM) is used to highlight the role of quantum interference in the tetraphenyl-aza-BODIPY central unit.

Introduction

The field of single-molecule electronics contains many studies of linear pseudo- one-dimensional molecular wires with a single anchor group at each end.[1-3] Such systems have been crucial for the understanding and development of molecular conductance owing to their ability to be modified in a modular fashion. However, to incorporate greater functionality, there is a need to explore how electricity flows through molecular structures with multiple anchor groups. The challenge is that as additional anchor groups are added to a molecule, the number of potential conductance paths increases, thereby increasing the complexity of the analysis. An early study of such molecules was performed by Grunder *et al*., whereby a 1,4-diethynyl-2,5-divinylbenzene motif was substituted by a combination of pyridyl and thiolate anchor groups, resulting in a system that could be electrochemically switched between conductive paths.[4] A second experimental study examined the conductance of 2,11-dithia[3.3]paracyclophane, in which the combination of two parallel conductive paths resulted in a conductance of 9.7×10^{-4} G_0.[5] This increase by a factor of 2.8 compared with the conductance of the equivalent single-path molecule, 1,4-bis[(methylthio)methyl]benzene (3.5×10^{-4} G_0) was a consequence of constructive quantum interference (QI).[5]

In the present study we seek to examine a significantly different system to that of Grunder *et al*.;[4] in which, rather than two conductive paths sharing a common conjugated core, two identical conductive parallel paths are held in close proximity, but are still linked by a conductive bridge. To realize such a structure, the tetraphenyl-difluoroboratriaza-indacene (tetraphenyl-aza-BODIPY) motif was chosen as it is a flat, rigid, highly conjugated molecule consisting of two 3,5-diaryl-substituted pyrrolates linked by a conjugated nitrogen and a BF_2^+ fragment (see Scheme 1). In addition to the low HOMO-LUMO energy gap, the 2,4-substitution pattern of the pyrrole has been shown by Yang to display destructive QI, while the 2,5-substituted analogue displayed none.[6]

Since the aza-BODIPY motif was first reported by Sathyamoorthi et al. in 1993,[7] these systems have been extensively studied due to their high near-infrared emission and biological stability,[8-11] which make them ideally suited as cellular stains. Furthermore, due to the work of O'Shea et al.,[12-14] their synthesis has become readily accessible. This present work examines the electrical conductance of the aza-BODIPY substituted with para-thioanisole moieties to give terminal thiomethyl anchor groups. This particular moiety was chosen as its symmetry limits any DQI effects to the aza-BODIPY core and the thioether contacts are known to favor mid-gap conductance.[15] For this motif, the HOMO is delocalized over the entire molecule whereas the LUMO is localized to the aza-BODIPY core.

Synthesis

The synthesis of target compounds **11** and **12** was according to O'Shea's procedure (see Scheme 1).[13-14] Following the synthesis of the chalcones (**1**-**3**) from 4-(methylthio)benzaldehyde and the corresponding ketone (acetophenone, 1-(4-(methylthio)phenyl)ethan-1-one or 1-(4-bromophenyl)ethan-1-one) via an aldol reaction, nitromethane was added via Michael addition to give **4**-**6**. The formation of the aza-DIPY's (**8** and **9**) was achieved by heating **5** and **6** with ammonium acetate in n-butanol. Although significant quantities of the crude precipitate were obtained, Soxhlet extractions were necessary to achieve sufficiently pure samples, resulting in the lower yields of 6 (**8**) and 37% (**9**). Conversion to their BF_2-chelates, **11** and **12**, was achieved by stirring $BF_3{\cdot}OEt_2$ with Et_3N and the corresponding aza-DPY (**8** and **9**).

Due to solubility limitations, the synthesis of **13** deviated from the established approach of Bouit et al. and Bellier et al.,[16-17] instead using Daddario et al.'s method,[18] performing a Sonogashira coupling on a bromo-substituted aza-DIPY precursor. Sonogashira coupling was

performed with 1-(4-bromophenyl)-3-(4-(methylthio)phenyl)-4-nitrobutan-1-one (**6**) and 4-ethynythioanisole to give 3-(4-(methylthio)phenyl)-1-(4-((4-(methylthio)phenyl)ethynyl)phenyl)-4-nitrobutan-1-one (**7**); the synthesis then followed O'Shea's approach to give the corresponding aza-DIPY (**10**) and aza-BODIPY (**13**). All compounds were fully characterized by ^{1}H, ^{13}C and ^{19}F NMR spectroscopy, high resolution mass-spectrometry or elemental analysis.

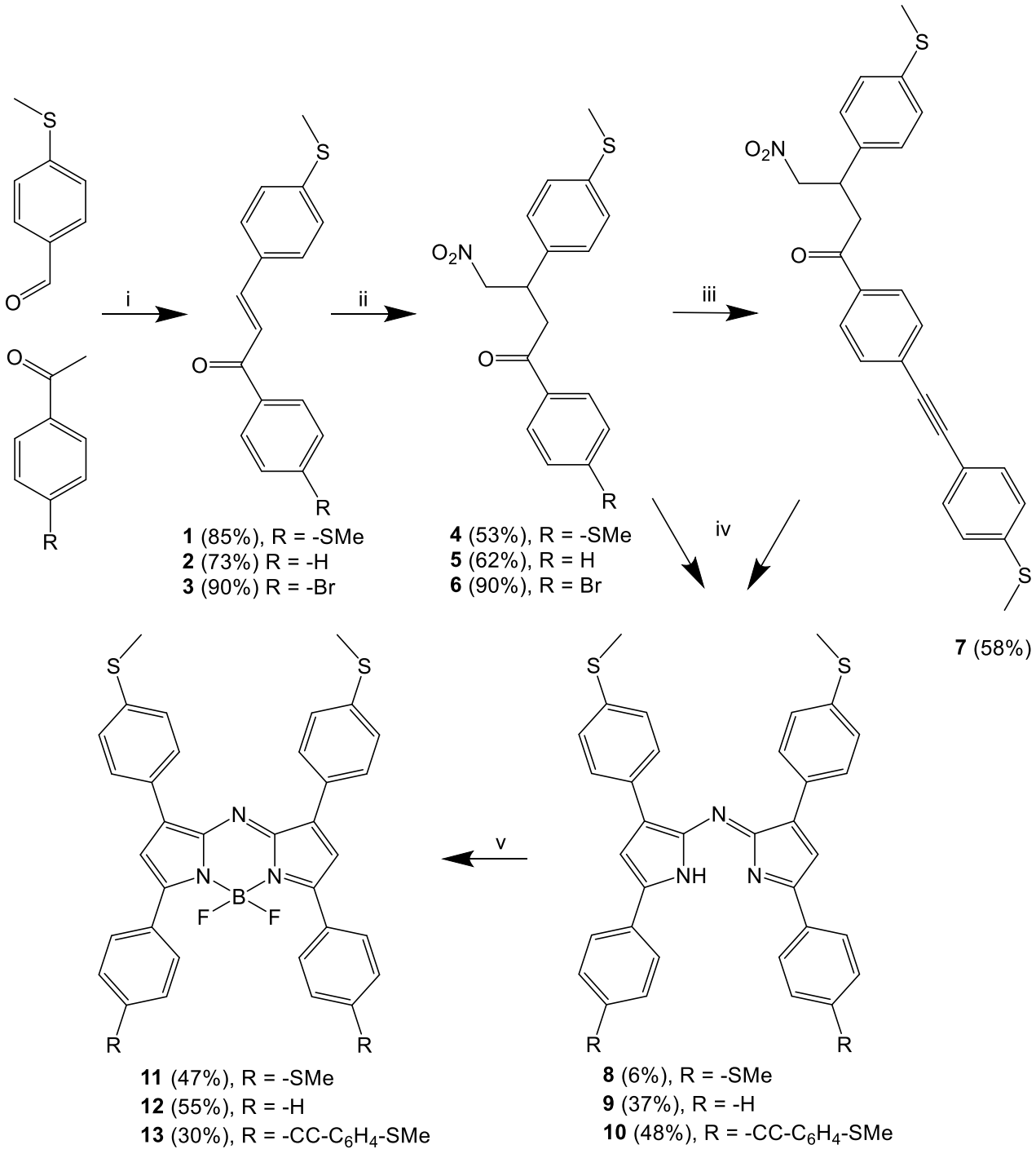

Scheme 1. Synthesis of substituted aza-BODIPYs using i) NaOH, H_2O/EtOH, ii) $MeNO_2$, MeOH, Et_2NH, iii), 4-ethynylthioanisole, $PdCl_2(PPh_3)_2$, CuI, Et_3N, THF, iv) NH_4OAc, n-butanol, v), $BF_3 \cdot OEt_2$, Et_3N, DCM.

Molecular Structures

Structures of **4**, **6**, **11**, **12**, and **13** were confirmed by single-crystal X-ray diffraction and were consistent with the obtained spectroscopic data. The molecular structures of **11-13** are shown in Figure 1. The central tricyclic moieties in these compounds show surprising conformational versatility; while that of **11** is planar within 0.07 Å, in **12** and **13** the dihedral angles between the planes of the two pyrrolyls (the folding angle along B…N line of the central cycles) are 24.3° and 22.1° respectively. Less surprising is a wide range of orientations of phenyl substituents, characterized by torsion angles around C(aza-BODPY)-C(Ph) bonds. In compounds **11-13** these angles vary from 12.6(8)° to 38.3(4)° for the distal (to the BF_2) pehnyl-group in **11** and **12** respectively. These values are in a good agreement with those found in the structures of 3-unsubstituted 2,4-diphenyl pyrroles (29 entries in the CSD), where distal-phenyl groups are inclined to be co-planar with pyrrole rings (the absolute values of corresponding torsion angles are below 35°). The molecule of the only known 3,5-unsubstituted 2,4-phenylpyrrole is virtually planar.[19]

The introduction of the second parallel conductive paths in the molecules **11-13** results in two likely contact orientations: straight (along the path) and diagonal (via the central heterocycle) ones. The average values of S...S distances for these two types of contacts are ca. 13.6 and 16.2 Å for molecule **11** and 20.4 and 22.9 Å for compound **13** respectively. Similar average S...p-H distances in molecule **12** are 12.9 and 15.3 Å for straight and diagonal paths respectively.

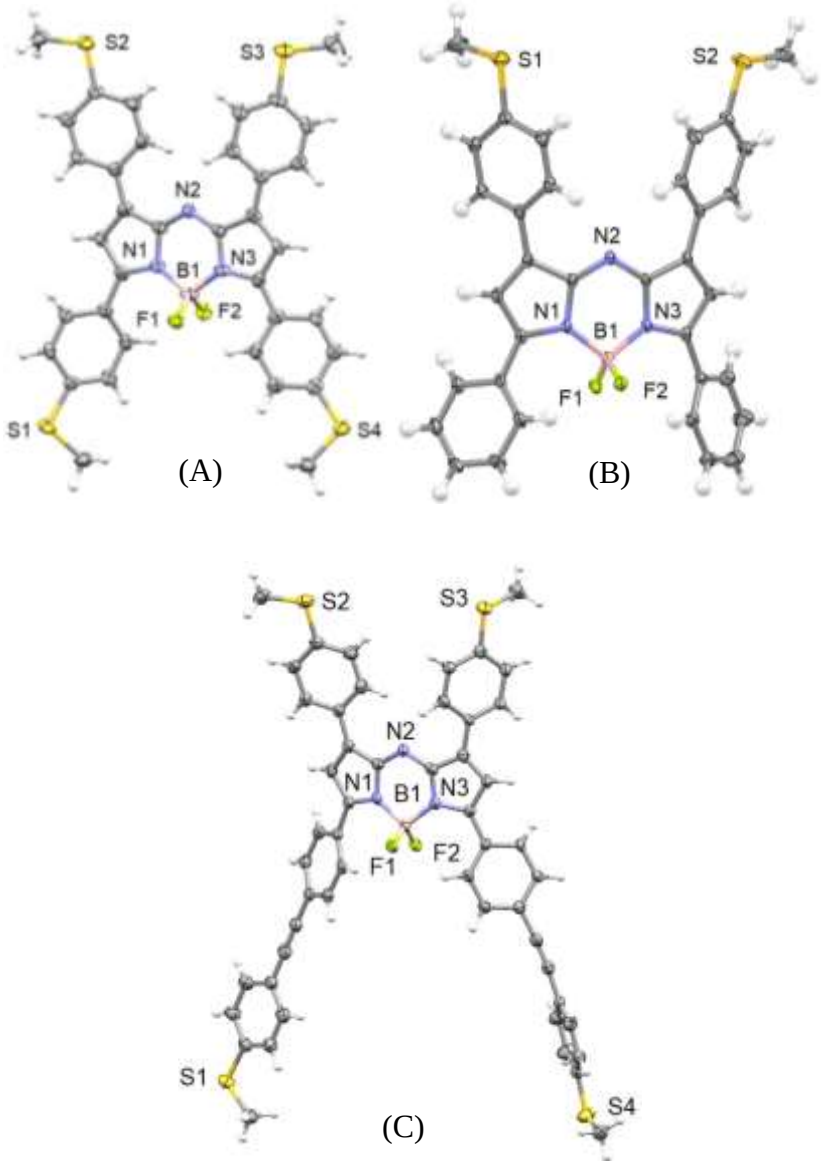

Figure 1. Crystal structures of **11** (A), **12** (B) and **13** (C), where the solvent molecule and disorder have been removed for clarity; thermal ellipsoids displayed at 50% probability.

Electrochemistry

The three new aza-BODIPYs (**11-13**) were characterized by cyclic and differential pulse voltammetry in DCM using a Fc/Fc^{+} internal reference. Redox potentials and frontier orbital

energies are given in Table 1. Each of the compounds (**11-13** and tetraphenyl-aza-BODIPY) displayed two separate reductions, at very similar potentials for the four molecules (± 0.04 V for the 1st reduction and ± 0.08 V for the 2nd) suggesting little effect on the LUMO and LUMO+1 due to changes in distal (to the boron) phenyl group substitution. For compounds **11** and **13**, two separate oxidations were observed, while only a single oxidation was observed for **12**. Such a difference suggests that the electron donation of the thiomethyl causes destabilization of the HOMO. This is reflected in the series of aza-BODIPY **12** and **11**; as the number of thiomethyl groups increases, the oxidation potential decreases. In the case of **13,** despite the molecule containing four thiomethyl groups, the inclusion of the alkyne between the proximal (to the boron) phenyl group and the thioanisole stabilizes the HOMO. These results suggest that while modifying the molecules in this fashion will alter any conductance paths involving the HOMO, any LUMO dominated paths will be unchanged.

Table 1. Electrochemical data for aza-BODIPYs **11-13**

Compound	**Oxidation Potential ($V_{Fc/Fc+}$)**		**Reduction Potential ($V_{Fc/Fc+}$)**		**HOMO (eV)**	**LUMO (eV)**	**LUMO+1 (eV)**
	1st	2nd	1st	2nd			
tetraphenyl-aza-BODIPY [20]	0.90		-0.81	-1.61			
11	0.51	0.79[a]	-0.85	-1.53	-5.374	-4.083	-3.390
12	0.73		-0.81	-1.58	-5.468	-4.028	-3.249
13	0.66	0.89[a]	-0.77	-1.43	-5.477	-4.068	-3.389

[a]Irreversible

Photochemistry

Aza-BODIPY compounds typically absorb and emit in the red to near-infrared region of the spectrum. Such low energy transitions are typically very sensitive to environmental effects, providing a means of modulating the energies of the frontier orbitals by varying the solvent. As such, the absorbance and emission spectra of the aza-BODPYs (**11-13**) were recorded in

solvents with different polarities, DCM (ε_r, 8.93), THF (ε_r, 7.60), EtOAc (ε_r, 6.02), $CHCl_3$ (ε_r, 4.81), and toluene (ε_r, 2.38), with solubility preventing measurements in cyclohexane and acetonitrile.

Each of the complexes displayed a $S_0 \rightarrow S_1$ band at 600–800 nm with $S_o \rightarrow S_2$ transition at 519–590 nm (see Figure 2);[18] this is significantly red-shifted relative to the parent aza-BODIPY and the methoxy analogue ($\lambda_{abs\ max}$ = 691 nm).[21] As the $S_0 \rightarrow S_1$ transition is purely HOMO→LUMO in character, a comparison can be made with the electrochemical data, showing approximately the same trend ΔE_{echem}|HOMO-LUMO| = **11**<**13**<**12** and absorbance ΔE_{abs}|HOMO-LUMO| = **13**≤**11**<**12**. Based on the electrochemical data, this is attributed to the electron donation of the thiomethyl group destabilizing the HOMO, with a limited effect on the LUMO. Given the $S_0 \rightarrow S_1$ transition offers a measure of the ΔE|HOMO-LUMO|, this can be used to examine the effect of solvent polarity on the frontier orbital energy. Comparing the solvent range of DCM→$CHCl_3$ for **11**, ΔE = 97 cm^{-1} and for DCM→toluene, ΔE = 177 cm^{-1} for **12** and 117 cm^{-1} for **13**, demonstrating a small but significant environmental effect on the frontier orbitals, if conductance were to occur via a sharp resonance near the Fermi energy such a variation in the ΔE|HOMO-LUMO| would likely result in a large change in conductance. In addition to the solvatochromic measurements, the photophysical measurements were completed with the determination of relative PLQYs and emission lifetimes, which were 0.32–0.71, significantly higher than that of similar 'simple' aza-BODIPYs; coupled with longer-than- usual emission lifetimes and red-shifted emissions (Table 2), this warrants further investigation.

Table 2. Photochemical data for aza-BODPYs **11-13**

Compound	**Absorption, nm ($\varepsilon \times 10^3$, L mol^{-1} cm^{-1})**	**S_1-S_0, eV**	**Emission, nm**	**Lifetime, ns**	**PLQY**
Aza-BOPY[21]	468 (6.0), 647 (85)		682	0.78	0.30

11	717 (93), 536 (25), 367 (sh,19), 326 (28), 272 (55)	1.618	758	2.6	0.71
12	672 (92), 535 (sh, 21), 312 (43), 270 (41)	1.717	735	1.7	0.32
13	717 (79), 552 (23), 379 (sh, 25), 331 (59), 288 (42)	1.633	761	2.0	0.47

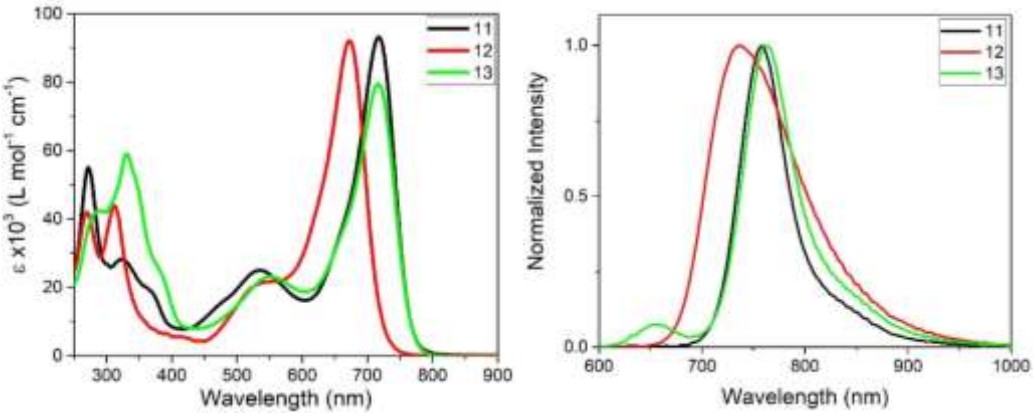

Figure 2. a) Absorption spectra of aza-BODPYs **11-13** recorded in DCM, and b) emission spectra of aza-BODPYs **11-13** recorded in DCM.

Conductance

The conductance of a series of compounds was measured using the BJ-STM technique and a THF/mesitylene solution (**11**, **12** and **13**), see Figure 3. Compounds **11** and **13** both show conductance peaks at 4.0×10^{-4} G_o and 2.5×10^{-5} G_o respectively. The lower conductance of **13** is consistent with the 0.6 nm increased length of **13**. The greater length of **13** is also reflected in an increased break-off distance, although the latter increase is less than the difference in molecular lengths, suggesting that the molecules may not be fully extended in the gold-molecule-gold junctions. This can be attributed to the stochastic nature of the junction breaking process, the fact that the thiomethyl group binds more weakly to gold than a thiol group and the degree of steric hindrance provided by the terminal methyl groups. As such, a distinction cannot be made between the contacts being made diagonally through the proximal and the distal phenyl rings and two pyrrole rings, or vertically through only the proximal and distal

phenyl rings and a single pyrrole ring. However, no conductance peak was evident for **12,** confirming that the conductance path does not pass through a proximal ring to the second proximal ring, therefore it is assumed that it cannot pass through both distal rings either. This is consistent with the break-off distance of both **11** and **13** being greater than the 0.7 nm S-S distance between either the distal or proximal pairs. Measurements were also performed in $CHCl_3$:air (depositing the compounds in $CHCl_3$ and measured in air), giving a lower hit rate but comparable conductance values of 2.1×10^{-4} G_0 (**11**) and 2.7×10^{-5} G_0 (**13**), with no conductance peak observed for **12**. Such variations in conductance with respect to solvent are common.[22]

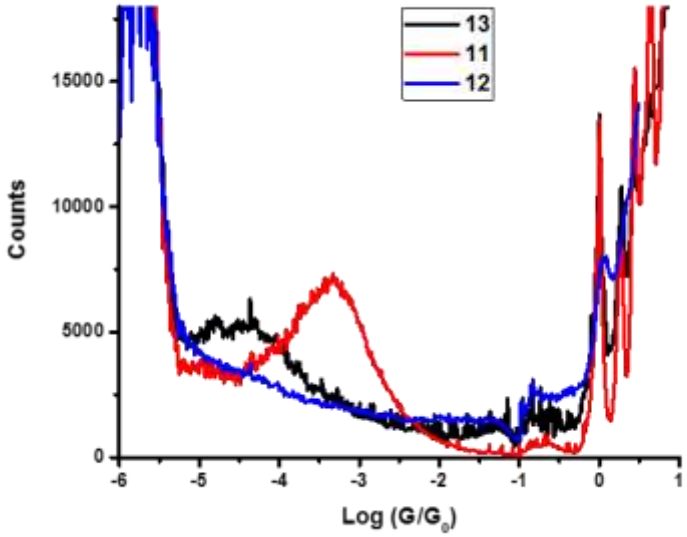

Figure 3. Conductance histograms of compounds **11-13** recorded in THF/Mesitylene

Table 3. Conductance values and break-off distances of compounds **11-13**

Molecule	Conductance (G/G_0)		Break-Off distance (nm)	
	THF/Mesitylene	$CHCl_3$/Air	THF/Mesitylene	$CHCl_3$/Air
11	4.0×10^{-4}	2.1×10^{-4}	1.4	1.4

13	2.5×10^{-5}	2.7×10^{-5}	1.6	1.6

Theory

We started by modelling the binding between terminal groups and Au, and then relaxed each compound in the presence of fixed leads. Using the density functional (DFT) code SIESTA[23], the optimum geometries of isolated **11**, **12** and **13** were obtained by relaxing the molecules until all forces on the atoms were less than 0.05 eV / Å (Figure S38). We used a double-zeta plus polarization orbital basis set, norm-conserving pseudopotentials, the local density approximation (LDA) exchange correlation functional, and in order to define the real-space grid, an energy cut-off of 250 Rydbergs. We also computed the results using GGA and found that the resulting transmission functions were comparable with those obtained using LDA.[24-25] To simulate the likely contact configuration during a break-junction experiment,[26-27] we employed leads constructed from 6 layers of Au (111), each containing 30 gold atoms, and further terminated with a pyramid of gold atoms in two junctions and flat leads in another junction (Figure 4). After relaxing each molecular junction in four different junction geometries, we calculated the electrical conductance using the Gollum quantum transport code.[28]

We performed DFT quantum transport calculations, exploring both the thiomethyl (Au-SMe) contact geometry and the Au-H direct contact. Figure S39 shows that **12** does not bind to gold through H atoms, which explains why **12** does not form a junction in the STM-BJ measurements. On the other hand, binding energy calculations for **11** and **13** suggest that they bind preferentially through their thiomethyl groups, and π-gold interactions are not favored. (Figures S40 and S41). This reduction in the π-stacked binding energy can be attributed to the torsional angles of the phenyl groups resulting in non-planar molecules, as shown in Figure 1.

As described in the SI (see Figure 4), four different junction geometries corresponding to different connectivities to gold electrodes were explored for each of **11** and **13.** The resulting transmission coefficients for these four geometries of **11** and **13** are shown in Figure S45.

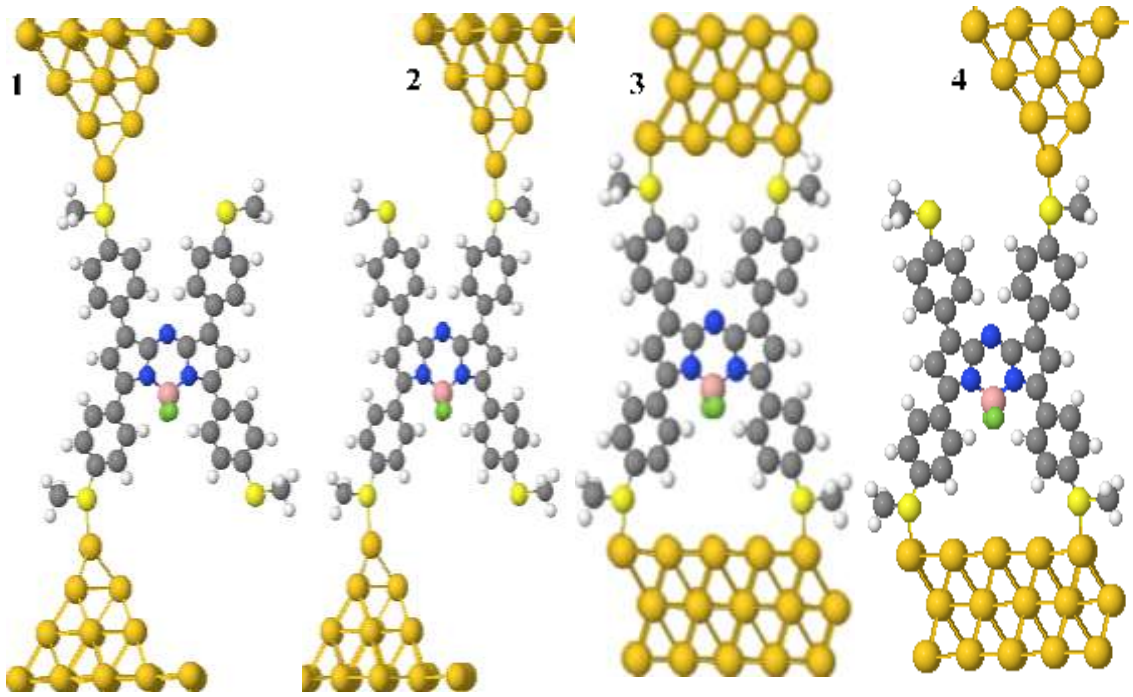

Figure 4. **11** in junctions, four possible geometries: 1, 2, 3 and 4 (respectively).

It is well known that DFT frequently underestimates the HOMO-LUMO gap[29-30][34,35] and from Table S16 in the Supporting Information it is clear that the calculated gaps are less than the optically-measured gaps. To overcome this deficiency, a scissor correction[31][36] is performed by diagonalizing the molecular sub-matrix of the full Hamiltonian, then shifting the eigenvalues above the Fermi energy such that the new HOMO-LUMO gap matches the experimental value of the isolated molecule, (see Table S16). Finally, the diagonalized matrix is transformed back to the original basis to obtain the corrected full Hamiltonian (for more details see[32-33][36-37]). Transmission coefficients after scissor corrections are shown in Fig. 5.

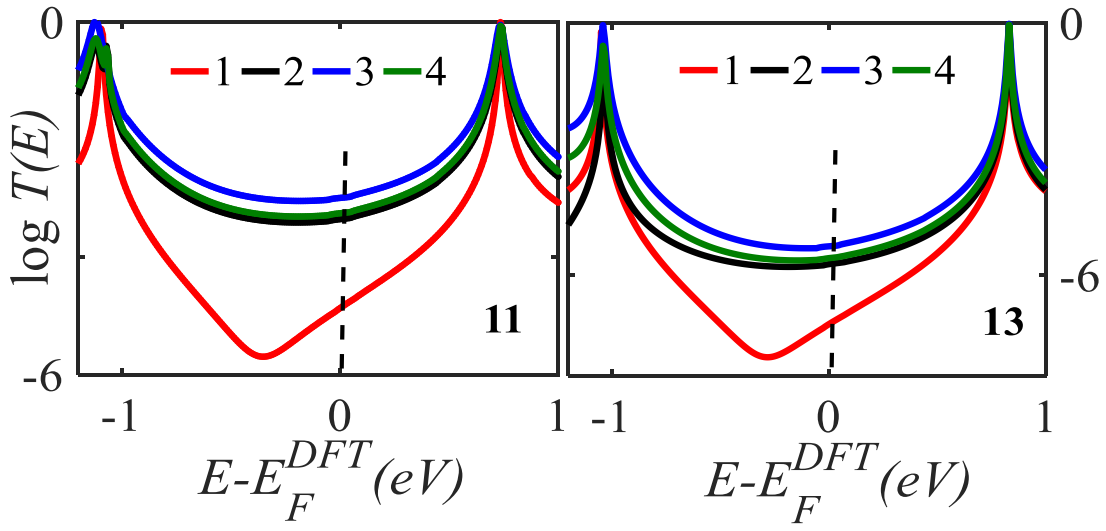

Figure 5. Transmission coefficients *T(E)* of **11** (left) and **13** (right) for four different possible geometries using scissors corrections (see Figure 4).

Figure 5 shows that connectivities 2, 3 and 4 produce constructive quantum interference (CQI) for both **11** and **13** (Figure 4), while geometry 1 yields destructive quantum interference (DQI), signified by the presence of a dip in the red curves near the middle of the HOMO-LUMO gaps (i.e. near E= –0.3eV). To obtain electrical conductances from these transmission curves, a value for the Fermi energy is needed. Literature comparisons between theory and experiment reveal that in the presence of nitrogen heteroatoms, DFT invariably predicts that the Fermi energy lies close to the LUMO resonance (as shown in Figure S45), whereas agreement with experiment is obtained only when the Fermi energy is chosen to be close to the middle of the HOMO-LUMO gap.[34-38][29-33] In agreement with these studies, we also find that the closest agreement between our theory and experiment is obtained for a Fermi energy located near the mid-gap, as indicated by the dashed lines in Figure 5. The corresponding room-temperature conductances are shown in Table 4. For comparison with experiment, Tables 4 also shows the average value of these four conductances of **11** and **13** ($E_F^{DFT} \approx$ mid gap).

To demonstrate that DQI is present in the π system of the aza-BODIPY core for connectivity 1, whereas CQI is present for connectivities 2-4, a simple tight binding model is presented in

the SI, which reproduces the qualitative features of DFT transmission curves (For more detail see section 10 of the SI).

Table 4. Experimental and theoretical conductance values of compounds **11**-**13** for the four geometries 1, 2, 3 and 4 shown in Figure 4. The theoretical values shown in parentheses are obtained without a scissor correction. Theoretical values obtained after a scissor correction are not enclosed by parentheses.

M	Conductance (G/G_0) Experiment		Conductance (G/G_0) for the four geometries Theory ($E_F^{DFT} \approx$ mid gap)				
	THF/Mesitylene	$CHCl_3$/Air	**1**	**2**	**3**	**4**	**Average**
11	4.0×10^{-4}	2.1×10^{-4}	(9.5×10^{-6}) 1.0×10^{-5}	(1.6×10^{-4}) 3.4×10^{-4}	(4.1×10^{-4}) 7.8×10^{-4}	(2.2×10^{-4}) 4.3×10^{-4}	(2.0×10^{-4}) 3.8×10^{-4}
13	2.5×10^{-5}	2.7×10^{-5}	(1.6×10^{-6}) 1.0×10^{-6}	(4.8×10^{-5}) 1.6×10^{-5}	(1.2×10^{-4}) 3.7×10^{-5}	(7.5×10^{-5}) 2.1×10^{-5}	(6.3×10^{-5}) 2.0×10^{-5}

CONCLUSION

We have measured and computed the electrical conductance of three closely related tetraphenyl-aza-BODIPY-based molecules. Molecules **11** and **13** with four thiomethyl anchors form stable contacts within our BJ-STM, with conductance values of $4.10^{-4}\,G_0$ and $2.5.10^{-5}\,G_0$, respectively. The lower conductance of the latter correlates with the increased length of **13** compared with **11**. On the other hand, **12**, having only two distal thiomethyl anchor groups, displayed no detectible conductance. Density functional theory-based calculations reveal that transport takes place through phase-coherent tunneling near the middle of the HOMO-LUMO gap. For each molecule, four connectivities to the thiomethyl anchors were considered, with three of the four exhibiting constructive quantum interference, with rather flat transmission functions near the gap center, and one exhibiting destructive interference, signified by a

transmission dip near the gap center. Although the measured electrical conductance reflects an average of all four possible connectivities, as shown in table 4, the low-conductance configurations corresponding to destructive quantum interference do not make a significant contribution to the average. Therefore, our study reveals that while transport through these molecules results from a combination of both constructive (involving the aza-BODIPY core) and destructive quantum interference (through the proximal and distal thioanisoles attached to the same pyrrole), the average conductance is dominated by configurations exhibiting constructive quantum interference. To highlight the role of quantum interference in the tetraphenyl-aza-BODIPY core, a simple tight binding model (TBM) was employed.

ASSOCIATED CONTENT

Supporting Information

Experimental procedures, NMR spectra, crystallographic, conductance details and computational details. Raw Break-Junction spectroscopy are available at the Data Catalogue: https://doi.org/10.17638/datacat.liverpool.ac.uk/973

AUTHOR INFORMATION

Corresponding Authors

*E-mail: ross.davidson@durham.ac.uk, andrew.beeby@durham.ac.uk, k.ismael@lancaster.ac.uk and nichols@liv.ac.uk

Notes

The authors declare no competing financial interest.

ACKNOWLEDGEMENTS

AB and RJD also gratefully acknowledge the EPSRC (EP/K007785/1; EP/K007548/1) for funding this work. DCM, RJN, CJL and SJH also gratefully acknowledge the EPSRC (EP/M029522/1; EP/M005046/1; EP/M014169/1; EP/N017188/1; EP/M014452/1) for funding this work. This work support from the European Commission is provided by the FET Open project 767187 – QuIET and the Iraqi Ministry of Higher Education (SL-20). A.K.I. acknowledges financial support from Tikrit University (Iraq). This work is also supported by the EC FP7 ITN "MOLESCO" project no. 606728.

REFERENCES

1. Hong, W.; Manrique, D. Z.; Moreno-García, P.; Gulcur, M.; Mishchenko, A.; Lambert, C. J.; Bryce, M. R.; Wandlowski, T., Single Molecular Conductance of Tolanes: Experimental and Theoretical Study on the Junction Evolution Dependent on the Anchoring Group. *Journal of the American Chemical Society* **2012**, *134*, 2292-2304.

2. Kaliginedi, V.; V. Rudnev, A.; Moreno-Garcia, P.; Baghernejad, M.; Huang, C.; Hong, W.; Wandlowski, T., Promising Anchoring Groups for Single-Molecule Conductance Measurements. *Physical Chemistry Chemical Physics* **2014**, *16*, 23529-23539.

3. Ashwell, G. J.; Urasinska, B.; Wang, C.; Bryce, M. R.; Grace, I.; Lambert, C. J., Single-Molecule Electrical Studies on a 7 Nm Long Molecular Wire. *Chemical Communications* **2006**, 4706-4708.

4. Grunder, S.; Huber, R.; Horhoiu, V.; González, M. T.; Schönenberger, C.; Calame, M.; Mayor, M., New Cruciform Structures: Toward Coordination Induced Single Molecule Switches. *The Journal of Organic Chemistry* **2007**, *72*, 8337-8344.

5. Vazquez, H.; Skouta, R.; Schneebeli, S.; Kamenetska, M.; Breslow, R.; Venkataraman, L.; Hybertsen, M. S., Probing the Conductance Superposition Law in Single-Molecule Circuits with Parallel Paths. *Nature Nanotechnology* **2012**, *7*, 663.

6. Yang, Y., et al., Heteroatom-Induced Molecular Asymmetry Tunes Quantum Interference in Charge Transport through Single-Molecule Junctions. *The Journal of Physical Chemistry C* **2018**, *122*, 14965-14970.

7. Sathyamoorthi, G.; Soong, M.-L.; Ross, T. W.; Boyer, J. H., Fluorescent Tricyclic B-Azavinamidine–Bf2 Complexes. *Heteroatom Chemistry* **1993**, *4*, 603-608.

8. McDonnell, S. O.; Hall, M. J.; Allen, L. T.; Byrne, A.; Gallagher, W. M.; O'Shea, D. F., Supramolecular Photonic Therapeutic Agents. *Journal of the American Chemical Society* **2005**, *127*, 16360-16361.

9. Killoran, J.; Allen, L.; Gallagher, J. F.; Gallagher, W. M.; O′Shea, D. F., Synthesis of Bf2 Chelates of Tetraarylazadipyrromethenes and Evidence for Their Photodynamic Therapeutic Behaviour. *Chemical Communications* **2002**, 1862-1863.

10. Zhou, E. Y.; Knox, H. J.; Reinhardt, C. J.; Partipilo, G.; Nilges, M. J.; Chan, J., Near-Infrared Photoactivatable Nitric Oxide Donors with Integrated Photoacoustic Monitoring. *Journal of the American Chemical Society* **2018**, *140*, 11686-11697.

11. Wang, Q.; Ng, D. K. P.; Lo, P.-C., Functional Aza-Boron Dipyrromethenes for Subcellular Imaging and Organelle-Specific Photodynamic Therapy. *Journal of Materials Chemistry B* **2018**, *6*, 3285-3296.

12. Loudet, A.; Bandichhor, R.; Burgess, K.; Palma, A.; McDonnell, S. O.; Hall, M. J.; O'Shea, D. F., B,O-Chelated Azadipyrromethenes as near-Ir Probes. *Organic Letters* **2008**, *10*, 4771-4774.

13. Gorman, A.; Killoran, J.; O'Shea, C.; Kenna, T.; Gallagher, W. M.; O'Shea, D. F., In Vitro Demonstration of the Heavy-Atom Effect for Photodynamic Therapy. *Journal of the American Chemical Society* **2004**, *126*, 10619-10631.

14. Wu, D.; O'Shea, D. F., Comparative Triad of Routes to an Alkyne-Bf2 Azadipyrromethene near-Infrared Fluorochrome. *Tetrahedron Letters* **2017**, *58*, 4468-4472.

15. Manrique, D. Z., et al., A Quantum Circuit Rule for Interference Effects in Single-Molecule Electrical Junctions. *Nature Communications* **2015**, *6*, 6389.

16. Bouit, P. A.; Kamada, K.; Feneyrou, P.; Berginc, G.; Toupet, L.; Maury, O.; Andraud, C., Two-Photon Absorption-Related Properties of Functionalized Bodipy Dyes in the Infrared Range up to Telecommunication Wavelengths. *Advanced Materials* **2009**, *21*, 1151-1154.

17. Bellier, Q.; Pégaz, S.; Aronica, C.; Guennic, B. L.; Andraud, C.; Maury, O., Near-Infrared Nitrofluorene Substitued Aza-Boron-Dipyrromethenes Dyes. *Organic Letters* **2011**, *13*, 22-25.

18. Daddario, C. M.; Han, Q.; Zeller, M.; Sauvé, G., Azadipyrromethene-Based near-Infrared Dyes: Effect of Thienylethynyl Substitution at the Distal and Proximal Phenyl Groups. *European Journal of Inorganic Chemistry* **2015**, *2015*, 3649-3657.

19. Chen, F.; Shen, T.; Cui, Y.; Jiao, N., 2,4- Vs 3,4-Disubsituted Pyrrole Synthesis Switched by Copper and Nickel Catalysts. *Organic Letters* **2012**, *14*, 4926-4929.

20. Gresser, R.; Hartmann, H.; Wrackmeyer, M.; Leo, K.; Riede, M., Synthesis of Thiophene-Substituted Aza-Bodipys and Their Optical and Electrochemical Properties. *Tetrahedron* **2011**, *67*, 7148-7155.

21. Bessette, A.; Ferreira, J. G.; Giguère, M.; Bélanger, F.; Désilets, D.; Hanan, G. S., Azadipyrromethene Dye Derivatives in Coordination Chemistry: The Structure–Property Relationship in Homoleptic Metal(Ii) Complexes. *Inorganic Chemistry* **2012**, *51*, 12132-12141.

22. Milan, D. C., et al., Solvent Dependence of the Single Molecule Conductance of Oligoyne-Based Molecular Wires. *The Journal of Physical Chemistry C* **2016**, *120*, 15666-15674.

23. Soler, J. M.; Artacho, E.; Gale, J. D.; Garcia, A.; Junquera, J.; Ordejon, P.; Sanchez-Portal, D., The Siesta Method for Ab Initio Order-N Materials Simulation. *Journal of Physics: Condensed Matter* **2002**, *14*, 2745-2779.

24. Ismael, A. K.; Wang, K.; Vezzoli, A.; Al-Khaykanee, M. K.; Gallagher, H. E.; Grace, I. M.; Lambert, C. J.; Xu, B.; Nichols, R. J.; Higgins, S. J., Side-Group-Mediated Mechanical Conductance Switching in Molecular Junctions. *Angewandte Chemie International Edition* **2017**, *56*, 15378-15382.

25. Herrer, I. L., et al., Unconventional Single-Molecule Conductance Behavior for a New Heterocyclic Anchoring Group: Pyrazolyl. *The Journal of Physical Chemistry Letters* **2018**, *9*, 5364-5372.

26. Fernández, M. A.; Sabater, C.; Dednam, W.; Palacios, J. J.; Calvo, M. R.; Untiedt, C.; Caturla, M. J., Dynamic Bonding of Metallic Nanocontacts: Insights from Experiments and Atomistic Simulations. *Physical Review B* **2016**, *93*, 085437.

27. Sabater, C.; Untiedt, C.; Palacios, J. J.; Caturla, M. J., Mechanical Annealing of Metallic Electrodes at the Atomic Scale. *Physical Review Letters* **2012**, *108*, 205502.

28. Ferrer, J., et al., Gollum: A Next-Generation Simulation Tool for Electron, Thermal and Spin Transport. *New Journal of Physics* **2014**, *16*.

29. Lof, R. W.; van Veenendaal, M. A.; Koopmans, B.; Jonkman, H. T.; Sawatzky, G. A., Band Gap, Excitons, and Coulomb Interaction in Solid ${\Mathrm{C}}_{60}$. *Physical Review Letters* **1992**, *68*, 3924-3927.

30. Hung, Y.-C.; Jiang, J.-C.; Chao, C.-Y.; Su, W.-F.; Lin, S.-T., Theoretical Study on the Correlation between Band Gap, Bandwidth, and Oscillator Strength in Fluorene-Based

Donor−Acceptor Conjugated Copolymers. *The Journal of Physical Chemistry B* **2009**, *113*, 8268-8277.

31. García-Suárez, V. M.; Lambert, C. J., First-Principles Scheme for Spectral Adjustment in Nanoscale Transport. *New Journal of Physics* **2011**, *13*, 053026.

32. Yzambart, G.; Rincón-García, L.; Al-Jobory, A. A.; Ismael, A. K.; Rubio-Bollinger, G.; Lambert, C. J.; Agraït, N.; Bryce, M. R., Thermoelectric Properties of 2,7-Dipyridylfluorene Derivatives in Single-Molecule Junctions. *The Journal of Physical Chemistry C* **2018**, *122*, 27198-27204.

33. Lambert, C. J., Basic Concepts of Quantum Interference and Electron Transport in Single-Molecule Electronics. *Chem. Soc. Rev.* **2015**, *44*, 875-888.

34. Wang, K.; Vezzoli, A.; Grace, Iain M.; McLaughlin, M.; Nichols, R. J.; Xu, B.; Lambert, C. J.; Higgins, S. J., Charge Transfer Complexation Boosts Molecular Conductance through Fermi Level Pinning. *Chemical Science* **2019**, *10*, 2396-2403.

35. Zang, Y.; Ray, S.; Fung, E. D.; Borges, A.; Garner, M. H.; Steigerwald, M. L.; Solomon, G. C.; Patil, S.; Venkataraman, L., Resonant Transport in Single Diketopyrrolopyrrole Junctions. *Journal of the American Chemical Society* **2018**, *140*, 13167-13170.

36. Gunasekaran, S.; Hernangómez-Pérez, D.; Davydenko, I.; Marder, S.; Evers, F.; Venkataraman, L., Near Length-Independent Conductance in Polymethine Molecular Wires. *Nano Letters* **2018**, *18*, 6387-6391.

37. Geng, Y.; Sangtarash, S.; Huang, C.; Sadeghi, H.; Fu, Y.; Hong, W.; Wandlowski, T.; Decurtins, S.; Lambert, C. J.; Liu, S.-X., Magic Ratios for Connectivity-Driven Electrical Conductance of Graphene-Like Molecules. *Journal of the American Chemical Society* **2015**, *137*, 4469-4476.

38. Garner, M. H., et al., Comprehensive Suppression of Single-Molecule Conductance Using Destructive Σ-Interference. *Nature* **2018**, *558*, 415-419.